Summation of Temporal L-Cone- and M-Cone-Contrast in the Magno- and Parvocellular Retino-Geniculate Systems in Glaucoma

Cord Huchzermeyer,[1,2] Folkert Horn,[1,2] Robert Lämmer,[1,2] Christian Mardin,[1,2] and Jan Kremers[1,2]

[1]Department of Ophthalmology, University Hospital Erlangen, Germany
[2]Friedrich-Alexander-University Erlangen-Nürnberg, Germany

Correspondence: Cord Huchzermeyer, Department of Ophthalmology, University Hospital Erlangen, Schwabachanlage 6, 91054 Erlangen, Germany; cord.huchzermeyer@uk-erlangen.de.

Received: December 19, 2020
Accepted: April 14, 2021
Published: May 14, 2021

Citation: Huchzermeyer C, Horn F, Lämmer R, Mardin C, Kremers J. Summation of temporal L-cone- and M-cone-contrast in the magno- and parvocellular retino-geniculate systems in glaucoma. *Invest Ophthalmol Vis Sci.* 2021;62(6):17. https://doi.org/10.1167/iovs.62.6.17

Purpose. The purpose of this study was to characterize summation of temporal L- and M-cone contrasts in the parvo- (P-) and magnocellular (M-) pathways in glaucoma and the relationship between the respective temporal contrast sensitivities (tCS) and clinical parameters.

Methods. Perifoveal tCS to isolated or combined L- and M-cone contrasts (with different contrast ratios, and therefore different luminance and chromatic components) were measured at different temporal frequencies (at 1 or 2 Hz and at 20 Hz) using triple silent substitution in 73 subjects (13 healthy, 25 with glaucoma, and 35 with perimetric glaucoma). A vector summation model was used to analyze whether perception was driven by the P-pathway, the M-pathway, or both. Using this model, L- and M-cone input strengths (A_L, A_M) and phase differences between L- and M-cone inputs were estimated.

Results. Perception was always mediated by the P-pathway at low frequencies, as indicated by a median phase angle of 179.84 degrees (cone opponency) and a median A_L/A_M ratio of 1.04 (balanced L- and M-cone input strengths). In contrast, perception was exclusively mediated by the M-pathway at higher frequencies (input strength not balanced: $A_L/A_M = 2.94$, median phase angles = 130.17 degrees). Differences in phase were not significant between diagnosis groups (Kruskal-Wallis = 0.092 for P- and 0.35 for M-pathway). We found differences between groups only for the M-pathway (L-cone tCS deviations at 20 Hz were significantly lower in the patients with glaucoma $P = 0.014$, with a strong tendency in M-cones $P = 0.049$). L-cone driven tCS deviations at 20 Hz were linearly correlated with perimetric mean defect (MD) and quadratically correlated with retinal nerve fiber layer (RNFL) thickness.

Conclusions. Unaltered phase angles between L- and M-cone inputs in glaucoma indicated intact temporal processing. Only in the M-pathway, contrast sensitivity deviations were closely related to diagnosis group, MD, and RNFL thickness, indicating M-pathway involvement.

Keywords: temporal contrast sensitivity, silent substitution, parvocellular system, magnocellular system, glaucoma

Glaucoma is a heterogeneous group of chronic-neurodegenerative diseases of the retinal ganglion cells and among the most common causes of blindness worldwide.[1,2] The current therapeutic approach of decreasing intraocular pressure[3,4] is often not sufficient, and the need for neuroprotective strategies is widely recognized.[5]

For the development and evaluation of such therapies, new tests of ganglion cell-related visual function are required that are more sensitive than the current gold standard,[6] which is standardized automated perimetry (SAP) of the central 30 degrees using a white Goldman III_4 stimulus on a white background.[7] Improved diagnostic performance has been achieved with several psychophysical methods that are supposed to isolate certain subpopulations of retinal ganglion cells (and their respective retino-geniculate pathways).[8,9]

The two dominant subpopulations of retinal ganglion cells in the human retina are the midget and the parasol ganglion cells, which differ in morphology, connectivity, receptive fields, spatial distribution, and physiological properties.[10,11]

The midget ganglion cells project to the parvocellular layer of the lateral geniculate nucleus (LGN; P-pathway) and are therefore also called P ganglion cells (P-GCs). They receive inputs from midget-bipolar cells and mediate red-green color vision by opponent L- and M-cone inputs.[11] Although most humans have more L- than M-cones, their inputs to the midget ganglion cells are balanced, probably due to synaptic weightings. Thus, sensitivities to L- and M-cone isolating stimuli are equal when perception is mediated by the P-pathway.[12] The P-pathway has a high spatial but low temporal resolution.

Copyright 2021 The Authors

This work is licensed under a Creative Commons Attribution-NonCommercial-NoDerivatives 4.0 International License.

The parasol ganglion cells project to the magnocellular layers of the LGN (M-pathway, M-GCs).[11] They transfer additive signals from L- and M-cones, resulting in a strong luminance sensitivity, and their input strengths are proportional to their packing densities. The M-pathway mediates luminance perception with a high temporal but low spatial resolution.[13]

The axons and cell soma of the MC ganglion cells might be more susceptible to glaucomatous damage because they are larger.[14] Although some studies found psychophysical evidence for such preferential damage,[15,16] other studies did not.[17–20] For the P-pathway, it seems that studies that use red-green contrast for isolation instead of high spatial / low temporal resolution tasks for isolation even found larger functional defects in the P-pathway.[21–23] Furthermore, it is not known whether any of these techniques might be able to demonstrate functional consequences of reduced synaptic density before ganglion cell death.[24,25]

We hypothesized that characterizing the processing of photoreceptor inputs in the retinal ganglion cells helps to clarify the mechanisms behind such conflicting results.

The properties of the P- and M-pathways can be assessed by using stimuli with different L- and M-cone contrast ratios.[26] Large luminance contrasts (to which particularly the M-pathway is sensitive) can be created by in-phase stimulation of the L- and the M-cones, large chromatic contrasts (to which the P-pathway is sensitive) by stimulation in counterphase. Most stimuli (including L- and M-cone isolating stimuli) will have a luminance and a chromatic component. It has been shown before that flicker detection thresholds for simultaneous stimulation of L- and M-cones can be predicted from the thresholds to single cone isolating stimuli based on a vector summation model.[27,28] The L- and M-cone isolating stimuli can be created using the silent substitution technique. The method has been described in detail before[29–31] and will be reviewed briefly in the Methods section.

It was the purpose of the present study to investigate (1) if detection thresholds of different combinations of L- and M-cone stimulation can be explained by the same vector summation model in patients with glaucoma and in healthy subjects, (2) how pathologic changes in glaucoma affect model parameters, and (3) how glaucomatous alterations in temporal contrast sensitivities relate to changes in retinal nerve fiber layer (RNFL) thickness and to SAP field sensitivity losses. In an earlier study, Alvarez et al.[32] used a very similar model for analyzing red-green contrasts, but they have not explicitly considered vector summation of the L- and M-cone inputs as the underlying mechanism and they have not validated their assumption that the major and minor axis of the fitted ellipses reflect activities of the P- and M-pathways.

Therefore, we examined flicker detection thresholds in an annular perifoveal test field for sinusoidal modulation of L- and M-cone isolating stimuli and for well-defined combinations of these in three groups: healthy subjects, glaucoma suspects without manifest visual field defects, and patients with perimetric glaucoma.

Methods

Subjects

Altogether, data from 73 subjects were included in this study. These data were collected in two series of measurements. The main series of measurements – using mixed L- and M-cone- stimuli with different L:M ratios (including L- and M-cone isolation) at 2 Hz and 20 Hz – was made in the year 2017, and data from these subjects were used in all analyses in this study (n = 57, 13 healthy subjects, 25 glaucoma suspects, and 19 patients with perimetric glaucoma; see Table 1). Healthy subjects were recruited among the staff of the University Hospital Erlangen and among healthy relatives of the participating patients with glaucoma.

In addition, data from another cohort of patients with glaucoma (Table 2) were used together with data from the first cohort for the comparison between contrast sensitivities and the clinical parameters perimetry and ocular coherence tomography (OCT) RNFL thickness. These data had already been obtained in 2015 (n = 20, 4 subjects had participated in both studies). All patients in this second cohort had perimetric glaucoma and visual field defects in the central 12 degrees, and only temporal contrast sensitivities to pure L- or M-cone-isolating stimuli at 1 Hz and 20 Hz were measured. Preliminary data from both series were shown at the annual ARVO conventions in 2016 and 2019.[33,34]

This study followed the tenets of the declaration of Helsinki and was approved by the Ethics committee of the medical faculty of the Friedrich-Alexander - University Erlangen - Nürnberg. All subjects gave written informed consent.

All patients with glaucoma participated in an ongoing longitudinal, observational study of glaucoma, the *Erlangen Glaucoma Registry*. Patients were examined annually under standardized conditions. Therapeutic decisions were made by the treating physicians independent of participation in the present study. Best-corrected visual acuity was measured with Snellen charts at a distance of 5 m and converted into logMAR. Further routine examinations included Haag-Streit slit lamp examination, indirect funduscopy with a 78-diopter-lens, and gonioscopy with a Goldman-three-mirror-lens.

Patients with congenital (X-chromosomal) color vision defects were excluded from the study. We considered a normal test Farnsworth Panel D15 result sufficient (saturated version). An anomaloscope examination was always performed if there were any errors in the D15 (Rayleigh equation, HMC anomaloscope; Oculus, Wetzlar, Germany) and also in the majority of subjects with a normal D15. Exclusion criteria were (1) presence of other retinal diseases, especially age-related macular degeneration, (2) diabetes mellitus independent of the presence of diabetic vasculopathy, (3) use of medications that impair visual function, and (4) clinically relevant cataract. An experienced ophthalmologist examined all subjects that were included in this study. Patients with diabetes mellitus were excluded because neural damage may precede diabetic vasculopathy. Normal age-related yellowing of the lens should not impair L- and M-cone isolating temporal contrast sensitivities according to calculations that we have previously published.[35]

Subjects were divided into three groups: (1) healthy subjects, (2) glaucoma suspects, and (3) perimetric glaucoma patients. Healthy subjects were characterized by an IOP of $\leq$ 21 mm Hg, normal Octopus G1 visual field (mean deviation ≤ -2 dB and absence of relevant focal defects, defined as 3 adjacent fields with a corrected probability of functional loss of $\geq$ 5%), and a normal morphology of the optic disc. Glaucoma suspects had normal visual fields, but had either ocular hypertension (IOD $\geq$ 21 mm Hg) or characteristic glaucomatous changes of the optic disc (cupping, focal defects of the neuroretinal rim, or the nerve fiber layer), or both. Patients with perimetric glaucoma had correlating optic disc changes and visual field defects. Differences in the

Table 1. Demographic and Clinical Data of the 2017 Cohort

	Healthy $N = 13$	Suspect $N = 25$	Perimetric $N = 19$	P. Overall	N
Age	54.0 (17.5)	62.1 (10.4)	70.9 (8.53)	0.001	57
Sex				0.608	57
M	7 (53.8%)	10 (40.0%)	7 (36.8%)		
F	6 (46.2%)	15 (60.0%)	12 (63.2%)		
BCVA (logMAR)	0.03 (0.04)	0.11 (0.20)	0.16 (0.10)	0.273	41
ONH classification (Jonas):				<0.001	50
0	13 (100%)	14 (63.6%)	0 (0.00%)		
1	0 (0.00%)	6 (27.3%)	2 (13.3%)		
2	0 (0.00%)	2 (9.09%)	8 (53.3%)		
3	0 (0.00%)	0 (0.00%)	5 (33.3%)		
VF: MD (G1, 30 degrees)	1.14 (0.68)	0.05 (1.88)	−5.89 (5.63)	<0.001	44
VF: $MD_{6\ degrees}$	1.35 (0.67)	0.57 (1.67)	−2.50 (2.50)	<0.001	41
VF: PSD	1.49 (0.35)	2.25 (1.16)	5.90 (2.99)	<0.001	45
OCT: total mean RNFL	97.3 (9.54)	86.8 (13.7)	60.5 (12.2)	<0.001	43
OCT: $RNFL_{6\ degrees}$	102 (11.6)	90.0 (19.2)	59.1 (11.1)	<0.001	40

BCVA, best corrected visual acuity; ONH, optic nerve hypoplasia; VF, visual field.

Table 2. Demographic Data From the Additional Perimetric Patients With Glaucoma From the 2015 Cohort

	Perimetric $N = 20$	N
Age	68.3 (7.47)	20
Sex		20
M	8 (40.0%)	
F	12 (60.0%)	
BCVA (logMAR)	0.10 (0.11)	18
ONH classification (Jonas):		17
0	1 (5.88%)	
1	1 (5.88%)	
2	12 (70.6%)	
3	3 (17.6%)	
VF: MD (G1, 30 degrees)	−8.31 (3.29)	18
VF: $MD_{6\ degrees}$	−2.96 (2.62)	18
VF: PSD	6.61 (2.50)	18
OCT: total mean RNFL	59.3 (10.5)	18
OCT: $RNFL_{6\ degrees}$	56.1 (16.0)	19

BCVA, best corrected visual acuity; ONH, optic nerve hypoplasia; VF, visual field.

visual field global indices ($P < 0.001$) and RNFL thicknesses ($P < 0.001$) between groups were a direct consequence of the group definitions, and therefore of no relevance. LogMAR was not significantly different between the groups. There were statistically significant age differences between groups (see Table 1; $P < 0.001$), which were addressed by correcting contrast sensitivities for age (see below).

LED Stimulator

We used a two-channel stimulator, each containing four differently colored LEDs as light sources, for creating photoreceptor-isolating stimuli using the triple silent substitution paradigm.[36] One channel can be used for central stimulation (circular with 2 degrees diameter); the second channels can be used to stimulate an annular field with 2 degrees inner and 12 degrees outer diameter. The soundcard of a personal computer was used to control eight LEDs (two red = 660 m; two green = 558 nm; two cyan = 516 nm; and two blue ones = 460 nm) with a very high temporal resolution.[37] The LED spectra were narrowed by interference filters to a bandwidth at half height of around 8 nm. Using a Maxwellian view-type optical pathway, we were able to achieve retinal illuminances up to 587 Td. Beam splitters and masks positioned in the pathway were used to create a circular field with a diameter of 2 degrees and a surrounding annular field with an outer diameter of 12 degrees. Calibration was carried out regularly according to previously published protocols.[12,38]

Stimulus

We used a very similar approach as described previously.[12,35,39,40] The stimulus is shown in Figure 1. Briefly, we used the annular outer field as the test field to display modulation. In the test field, the mean LED luminances were always set so that the retinal illuminance was 294 Td and the chromaticity was white with CIE coordinates of x = 0.38 and y = 0.28. During the experiments, the LED luminances were modulated around these means without changing the time-averaged retinal illuminance and chromaticity. As a consequence, the retinal adaptation remained constant. The central circular field was used as a fixation target and was not modulated. Retinal illuminance was 147 Td and the chromaticity was equal to that of the test field.

Temporal modulation of the test field was sinusoidal, and we measured both at a low temporal frequency (either 1 Hz in the 2015 cohort or 2 Hz in the 2017 cohort) and at a high temporal frequency (20 Hz in both cohorts).

Silent Substitution

Briefly, the photoreceptor types differ in their spectral sensitivity, that quantifies the probability that a photon of a given wavelength is absorbed. However, the principle of univariance[29] states that the reaction of the photoreceptor is always the same independent of the photon's wavelength. Thus, when two stimuli of different spectral compositions are exchanged, differences in a photoreceptor's sensitivity to the stimuli can be compensated by choosing appropriate intensities. For instance, an exchange between two stimuli, one containing short wavelengths and the other long wavelengths, may not result in a modulation of L-cone excitation when the short wavelength stimulus is more intense than the long wavelength stimulus. However, the same stimulus will strongly stimulate the M-cones. In that case, the response of

Investigative Ophthalmology & Visual Science

Table 3. Parameters Used for Data Analysis and How They Were Calculated

Symbol	Parameter	Processing
C	(Michelson) contrast at threshold	$(I_{max} - I_{min}) / (I_{max} + I_{min})$
CS/logCS	Contrast sensitivity/Log contrast sensitivity	1/C
$A_{L/M}$	Model parameters of L- and M-cone input strength	theoretically identical to $CS_{L/M}$
$CSD_{L/M}$ [dB]	Contrast sensitivity deviations	$\log CS_{patient} - \log CS_{normal}$
$MD_{6\ degrees}$ [dB]	Mean deviation values of 8 VF locations	Locations 23, 24, 28, 29, 32, 33, 38, 39; defects were anti-logged for averaging
$RNFL_{6\ degrees}$ [µm]	OCT retinal nerve fiber layer thickness	Sectors 2, 3, 4, 5, 28, 30, and 31 averaged

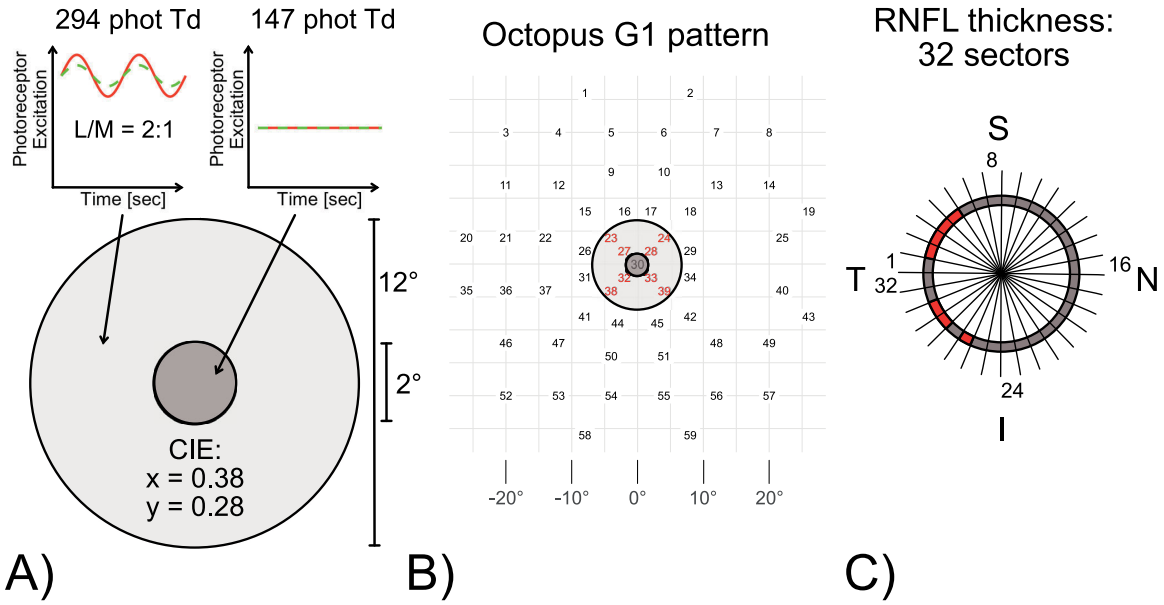

Figure 1. Schematic illustration of the spatial and temporal structure of the stimulus used for temporal contrast sensitivity measurements and how its spatial structure relates to OCT and SAP field. Panel (**A**) shows the annular test field (outer diameter 12 degrees and inner diameter 2 degrees), its time-averaged retinal illuminance and its CIE coordinates. Chromaticity and luminance were temporally modulated, but the average remained constant and was identical for all stimulus conditions. The central circular field had the same CIE coordinates, but a 50% lower retinal illuminance. It was not modulated and served as a fixation target. Panel (**B**) shows how the spatial structure of the stimulus relates to the G1 pattern of the Octopus 900 visual field. The antilogarithms of the defect values in the eight locations which coincide with the annular test field (marked in red) were averaged for calculating the $MD_{6\ degrees}$. Panel (**C**) shows the 32 sectors of the OCT RNFL measurements. The sectors marked in *red* were averaged for the $RNFL_{6\ degrees}$ value.

any system that exclusively or mainly receives L- and M-cone input (as the M- and P- pathways at photopic conditions) will be mediated by the M-cones. When four primaries with different wavelength contents are used, perfect isolation of each of the four photoreceptor types can be achieved by varying intensity of all four primaries (triple silent substitution) at identical states of retinal adaptation.[29,30]

We previously validated that photoreceptor isolation is feasible.[12,35,39] As mentioned above, L- and M-cone isolating stimuli contain both a luminance and a chromatic component and detection thresholds were mediated by the P-pathway at low and by the M-pathway at high temporal frequencies.[12,41]

Using matrix calculation, modulation contrasts and phases (either in-phase or counter-phase) of the LEDs were calculated based on the spectral sensitivities of the photoreceptors in a way that L- and M-cones were stimulated at different L:M contrast ratios (again, either in-phase or counter-phase), whereas contrasts in S-cones and rods were either zero (silent substitution) or at least negligible (because of variability e.g. in pigment spectra or preretinal absorption[35]). The LED contrasts and phases that we used are shown in the Supplementary Table S1, together with the resulting contrasts at the photoreceptor level.

Photoreceptor-isolating temporal modulation thresholds were measured at a convenient time during a visit for the standardized routine examinations. Measurements were carried out in a separate, calm, and dimly lit room. All subjects were adapted to the room light for at least 15 minutes prior to measurements. We measured the more severely affected eye unless there were exclusion criteria, and we chose the right eye when there was no relevant difference between eyes. The fellow eye was occluded with a transparent eyepatch and the subjects were positioned in front of the LED stimulator. Breaks were taken every 15 minutes.

We have described psychophysical threshold determination in detail before.[12] In brief, we used a PEST strategy with two randomly interleaved staircases. One staircase started at 0%, the other at 100% contrast.

In the 2015 cohort, only thresholds to pure L- and M-cone isolating stimuli were measured (L:M ratios of 1:0 and

Investigative Ophthalmology & Visual Science

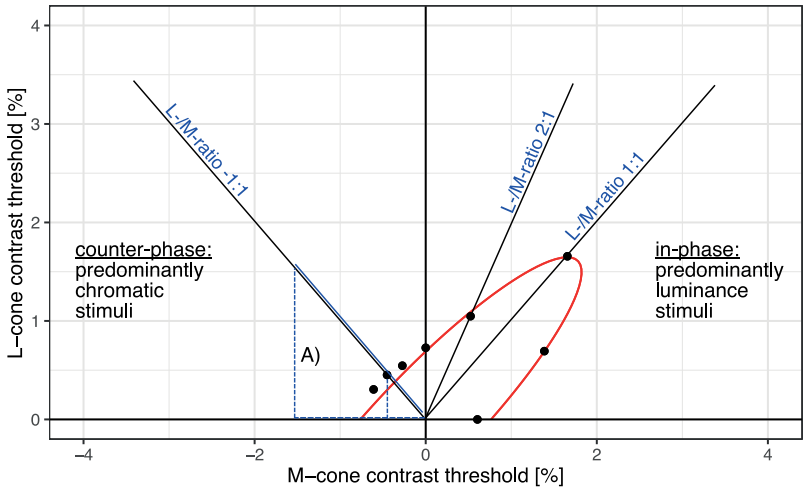

Figure 2. Exemplary fit of an elliptic vector summation model to the temporal contrast perception thresholds for mixed L- and M-cone-isolating stimuli with different L:M ratios. The *closed circles* represent the measured M-cone- and L-cone-contrasts at threshold. Points on the same straight line through the origin have the same L:M ratio (see *blue triangles* marked with an A). The larger the distance between the data point and the origin, the larger the contrast for flicker detection threshold and thus the lower the sensitivity. If the thresholds fall on an ellipse, they can be described by a vector summation of the incoming L- and M-cone signals. The red ellipse represents the model fit (Equations 1 and 2).

0:1). In the 2017 cohort, at least four out of eight ratios were measured (1:0, 0:1, 1:1, 1:-1, 1:2, 2:1, 1:-2, and 2:-1; negative ratios indicate counterphase modulation).

Modeling the Interaction Between L-Cone- and M-Cone-Inputs

If the contrast thresholds for mixed L- and M-cone stimuli can be described by vector summation of the L- and M-cone inputs with a phase lag, the measured thresholds are located on an ellipsis around the origin in a plot where L-cone contrast C_L is plotted against M-cone contrast C_M (Fig. 2).[14,24,25]

Our vector summation model is based on the following equations, which calculate C_L and C_M for a given L:M ratio ($K = \frac{C_L}{C_M}$). For pure L-cone isolating stimuli, $C_M = 0$ and $C_L = \frac{1}{A_L}$. For all other ratios, the following equations are used:

$$C_M = \frac{1}{\sqrt{A_L^2 \cdot K^2 + 2 \cdot A_L \cdot A_M \cdot K \cdot \cos\Delta\alpha + A_M^2}} \quad (1)$$

and

$$C_L = K \cdot C_M. \quad (2)$$

The model parameters are A_L and A_M, which represent the sensitivities of the two photoreceptor types, and $\Delta\alpha$, which is the phase lag between both. For pure L- or M-cone-isolating stimuli, contrast sensitivities (CS) were defined as the inverse of the threshold contrast for that photoreceptor type. Thus, according to the equations above, the contrast sensitivities CS_L and CS_M for these stimuli would equal the model parameters A_L and A_M for a perfect model fit.

Nonlinear least-squares estimate for the model parameters were obtained using the nlsLM function of the R-package minpack.lm. The underlying nonlinear function returned the cartesian distance of a threshold from the origin ($\sqrt{C_L^2 + C_M^2}$) as a function of K based on the equations shown above.

We have excluded measurements where observers were not able to perceive maximally possible stimulus contrasts, because this would have resulted in floor effects of the resultant sensitivities. If less than four points were available for analysis, a model fit was not performed (NA values).

Visual Fields

An Octopus 900 perimeter (Haag-Streit, Köniz, Switzerland) with the G1 pattern (consisting of 59 locations in the central 30 degrees) was used to measure the visual field. In some of the healthy subjects, only the TOP strategy was used to ascertain that visual fields were normal. These fields were not analyzed further. In the patients with glaucoma and the healthy subjects who underwent the extended routine examination as participants in the Erlangen Glaucoma Registry study, two full-threshold measurements were performed. In addition to the standard global parameters (mean defect [MD] and pattern standard deviation [PSD]), mean deviation in the locations that coincided with the annular test field of the LED stimulator ($MD_{6\ degrees}$) was calculated by averaging the antilogarithm of the defect values for 8 (out of 59) Octopus G1 field locations (23, 24, 28, 29, 32, 33, 38, and 39) and subsequently calculating the logarithm of this average. For these calculations, data were exported from the Haag-Streit EyeSuite software and analyzed with the R statistical programming language and the visualFields package.[42]

Ocular Coherence Tomography

Peripapillary RNFL thickness was measured using spectral domain ocular OCT with the HRA system (Heidelberg Engineering, Heidelberg, Germany). We averaged the RNFL thickness from sectors that contribute to the test field by averaging the RNFL thickness of 7 out of 32 sectors ($RNFL_{6\ degrees}$).

Investigative Ophthalmology & Visual Science

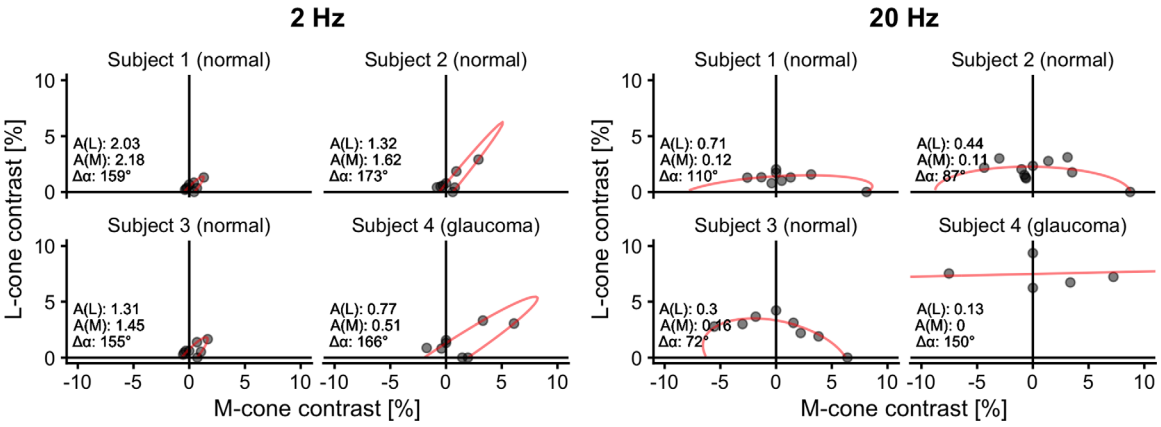

Figure 3. Vector summation model fits for different subjects at 2 Hz and 20 Hz. Subjects 1 to 3 were healthy observers, whereas subject 4 was a glaucoma patient. The model is explained in Figure 2. Model parameters A_L, A_M, and $\Delta\alpha = \alpha_L - \alpha_M$ are given in the insets.

These were sectors 2, 3, 4, 5, 28, 30, and 31, where sector 1 is located just above the temporal horizontal hemi-meridian and sectors are numbered clockwise.

Data Analysis

Temporal contrast sensitivity deviations were calculated from the contrast thresholds with the purpose of facilitating comparisons with clinical markers by subtracting the median of the $\log_{10}$ of the healthy subjects' contrast sensitivities (logCS) from the observed logCS values (see Table 3). To account for age differences between groups (see Table 1, $P < 0.001$), we performed an age correction on the logCS measurements according to a model that we established in an earlier study.[40] This model assumes a loss of 0.01 logCS per year. Then, sensitivity deviations were converted to decibel (dB). By definition, loss of sensitivity was represented by negative values.

We used the Kruskal-Wallis test for identifying significant differences between groups and the Wilcoxon test for pairwise comparison (with Holms correction for multiple testing). Because only one eye from each subject was included, correlated measurements were a minor issue.

Linear and quadratic regression models were fit in order to describe sensitivity deviations as a function of either $MD_{6\ degrees}$ or $RNFL_{6\ degrees}$. Only models that were significant after correction for multiple testing are shown, and quadratic regression was reported instead of linear regression if the coefficient for the quadratic term was significant at $P < 0.05$ (similar to Garway-Heath et al.[43]).

Results

Modeling Contrast Thresholds for Mixed L- and M-Cone-Isolating Stimuli

In 3 healthy subjects and one glaucoma suspect from the 2017 cohort, contrast thresholds measurements were performed for 8 different L:M ratios (see Fig. 3). At both 2 Hz and 20 Hz, we were able to describe contrast sensitivity by the above-mentioned model based on vector summation.

At 2 Hz, contrast thresholds were generally lower (and sensitivities were thus higher) than at 20 Hz. This corresponds to a position closer to the origin in Figure 3. For all 4 subjects, the fits to the 2 Hz data revealed that $\Delta\alpha$ was close to 180 degrees at 2 Hz and that A_L and A_M had similar values (thus, the ratios $\frac{A_L}{A_M}$ were close to 1). Altogether, the model fits were excellent at 2 Hz (residual sum of squares = median 0.07, and range = [0.0008 to 25.4]).

In contrast, at 20 Hz, as mentioned above, values for A_L and A_M were generally smaller than at 2 Hz, there were marked interindividual variabilities in the phase angles, and model fits were poorer (residual sum of squares: median 0.25, range = [0.006 to 13.3], Wilcoxon $P = 0.038$ compared with 2 Hz). In all 4 cases shown in Figure 3, the estimated L-cone-driven sensitivity (A_L) was higher than that driven by the M-cones (A_M) and thus the ratios $\frac{A_L}{A_M}$ were larger than 1. Compared with the three healthy subjects, the glaucoma subject had much higher thresholds and thus smaller A_L and A_M values at 2 and 20 Hz.

For the rest of the 2017 cohort, we determined contrast thresholds for four different L:M stimulation ratios (0:1, 1:0, 1:1, and 1:-1). The results of the model fits are shown in Figure 4. Despite the limited number of data points, model fits were generally satisfactory. At 2 Hz, the estimates for the parameters A_L and A_M were, again, very similar to each other for each subject (median L:M ratio = 1.04), and the phase angles were close to 180 degrees (median phase angle = 179. 84; see Fig. 4, top panels), regardless of diagnosis group (Kruskal-Wallis: $P = 0.092$). This confirms mediation of temporal contrast perception by the parvocellular system. Indeed, the subjects reported substantial chromatic changes in the test field close to threshold.

At 20 Hz, the subjects were more sensitive for L-cone than for M-cone stimuli in most cases (median L:M ratio = 2.94). Phase angles $\Delta\alpha$ were much more variable but generally substantially smaller than 180 degrees (median = 130.17 degrees; see Fig. 4, bottom panels). Again, this was the case for all groups. This is in agreement with the notion that thresholds were mediated by the magnocellularly based luminance channel and by the fact that the subjects reported that at threshold they perceived achromatic flicker. Although the absolute sensitivities were lower at high temporal frequencies compared to low temporal frequencies, the subjects generally reported to be more certain about their answers.

There were no significant differences in phase angle between diagnosis groups (Kruskal-Wallis test: $P = 0.092$ for 2 Hz and $P = 0.35$ for 20 Hz). Furthermore, there were excellent correlations between the model parameters A_L and A_M on the one hand and the observed contrast sensitivities for pure L- and M-cone isolating stimuli (CS_L and CS_M) on

Investigative Ophthalmology & Visual Science

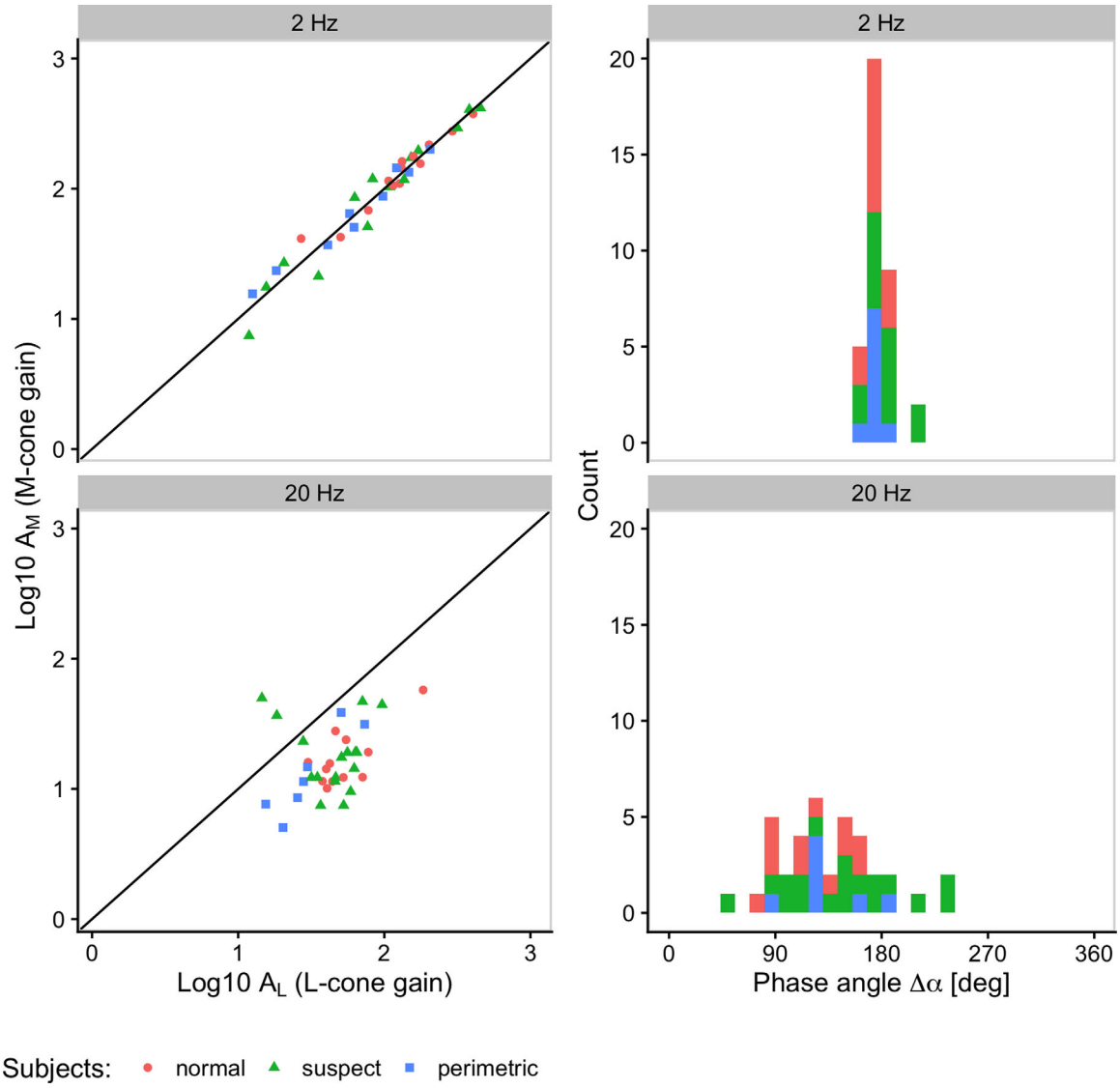

Figure 4. Parameter estimates of the vector summation model in the subjects from the 2017 cohort. On the left, L-cone-sensitivity (A_L) is plotted against M-cone sensitivity (A_M) for each subject. The *black lines* represent equal sensitivities. At 2 Hz, L- and M-cone-driven sensitivities were almost identical. At 20 Hz, M-cone-driven sensitivities were lower than L-cone-driven sensitivities. On the right, the phase angle estimates are plotted as histograms. There were no obvious phase angle differences between the diagnosis groups at 2 Hz. At 20 Hz, phase angles have a much larger interindividual variability, and there were no obvious differences between the groups.

the other hand. This confirmed the theoretical relationship from the above equations and highlighted the quality of the model fits (Spearman Rho: 0.90 for L-cones 2 Hz, 0.97 for L-cones 20 Hz, 0.95 for M-cones 2 Hz, and 0.98 for M-cones 20 Hz, $P < 0.001$ in all cases). Therefore, we decided to use the L- and M-cone contrast sensitivities (converted to sensitivity deviations in dB) because this allowed us to include data from patients with perimetric glaucoma measured in 2015.

L-Cone and M-Cone Sensitivities in the Subject Groups

In 2015, the low frequency measurements were performed at 1 Hz, but according to previous studies, sensitivities at 1 Hz and at 2 Hz are quite similar.[12] We used a model for age correction that we developed in an earlier study.[40]

The sensitivity deviations for the different diagnosis groups are shown in Figure 5. At high temporal frequencies, there was a statistically significant loss of temporal contrast sensitivity in the perimetric glaucoma group.

As mentioned before, the losses were age corrected. We also recalculated the expected differences assuming a larger age-related loss of 0.15 dB/year instead of 0.1 dB/year, because confidence intervals for this slope indicated a 5% probability of an age effect of 0.15 or larger, but the differences between groups remained significant (Kruskal-Wallis $P = 0.041$ instead of 0.014 after correction for multiple testing).

At low temporal frequencies, photoreceptor-isolating sensitivity deviation values were quite variable, and there was considerable overlap between the different diagnosis groups. There was a tendency toward a sensitivity loss in the glaucoma suspects with four glaucoma suspects showing

Investigative Ophthalmology & Visual Science

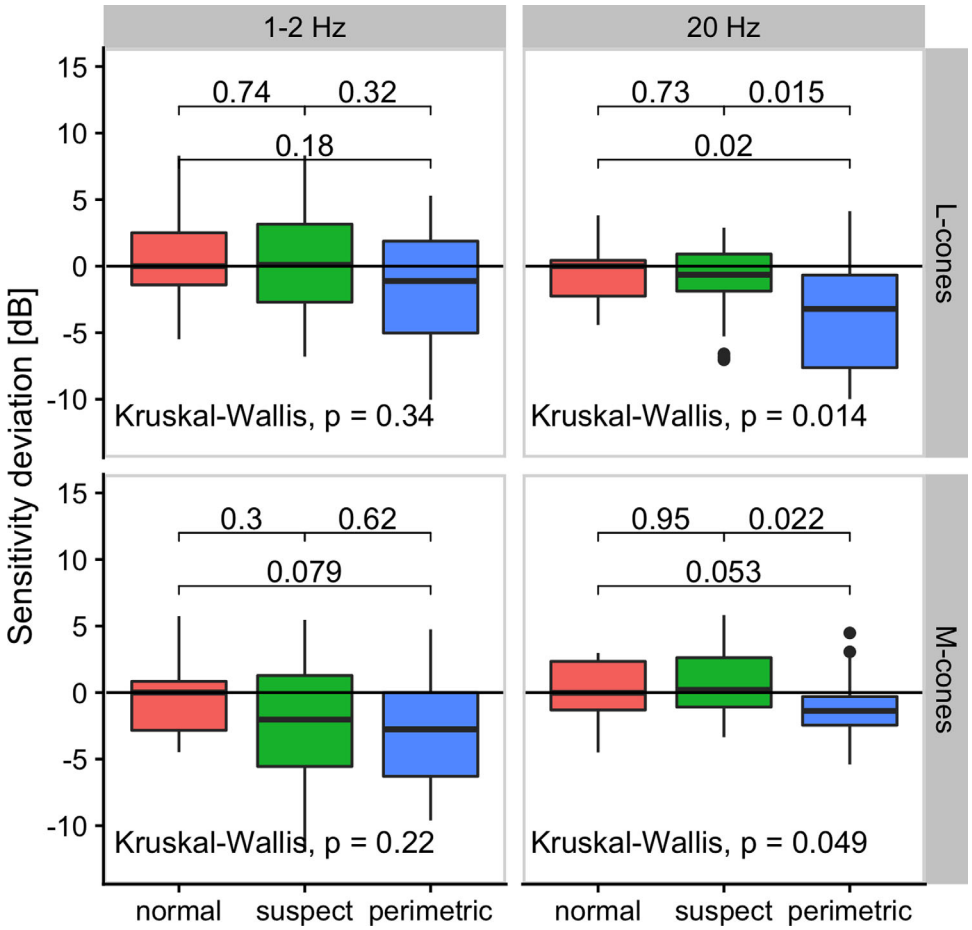

Figure 5. Sensitivity deviations for pure L-cone- or pure M-cone-isolating stimuli mediated by the parvocellular system (1-2 Hz) and by the magnocellular system (20 Hz). Subjects from both cohorts were included. Sensitivity deviations were calculated by subtracting the logarithm of the contrast sensitivity (logCS) from the median of the logCS in the normal group, and then converting to dB. Negative values indicate a loss of sensitivity. All logCS values were adjusted for age.

substantial sensitivity losses, despite normal visual acuity, visual field, and anomaloscope findings (Rayleigh equation).

Parvo- Versus Magnocellular Pathway

A paired *t*-test of the L-cone data showed that, on average, the mean sensitivity deviation at low temporal frequencies (P-pathway) was more negative than at high frequencies (M-pathway) with $P < 0.05$. For the M-cones, the difference was not significant ($P = 0.075$).

Comparison With Clinical Parameters (Both Cohorts)

Figure 6 shows the relationship between sensitivity deviation and clinical parameters. There were statistically significant relationships between L-cone-driven sensitivity deviations at high frequencies and $MD_{6\ degrees}$ (linear regression: $R^2 = 0.256$, $P < 0.001$ after Holms correction for multiple testing) as well as $RNFL_{6\ degrees}$ (quadratic regression: $R^2 = 0.279$, $P < 0.001$ after correction, $P = 0.02$ for the quadradic coefficient). Regression analysis was not significant for M-cone sensitivity alterations at high frequencies, probably because the dynamic range of the measurements were reduced with M-cone isolating stimuli. There was a significant linear relationship between M-cone-sensitivities at low frequencies and $MD_{6\ degrees}$ (linear regression: $R^2 = 0.085$, $P < 0.001$ after correction for multiple testing). The overall relationship between photoreceptor-specific sensitivity deviation and $RNFL_{6\ degrees}$ was similar to the relationship between $MD_{6\ degrees}$ and $RNFL_{6\ degrees}$ (quadratic regression: $R^2 = 0.596$, $P < 0.001$, $P = 0.001$ for the quadradic coefficient).

Discussion

Our data show that retinal processing in glaucoma patients can be characterized using combined L- and M-cone-isolating stimuli. The model, which assumes vector addition of the photoreceptor signals in the retinal ganglion cells, can indeed describe flicker detection thresholds for such stimuli. The data indicate that all stimuli – regardless whether chromatic or luminance contrast was dominant – were detected by the P-pathway at low and by the M-pathway at high temporal frequencies. We did not find evidence for relevant changes in retinal processing in glaucoma. Altogether, this implies that the sensitivities to temporal L- and M-cone contrasts can be used as parameters for functional changes in these systems. Among these

Investigative Ophthalmology & Visual Science

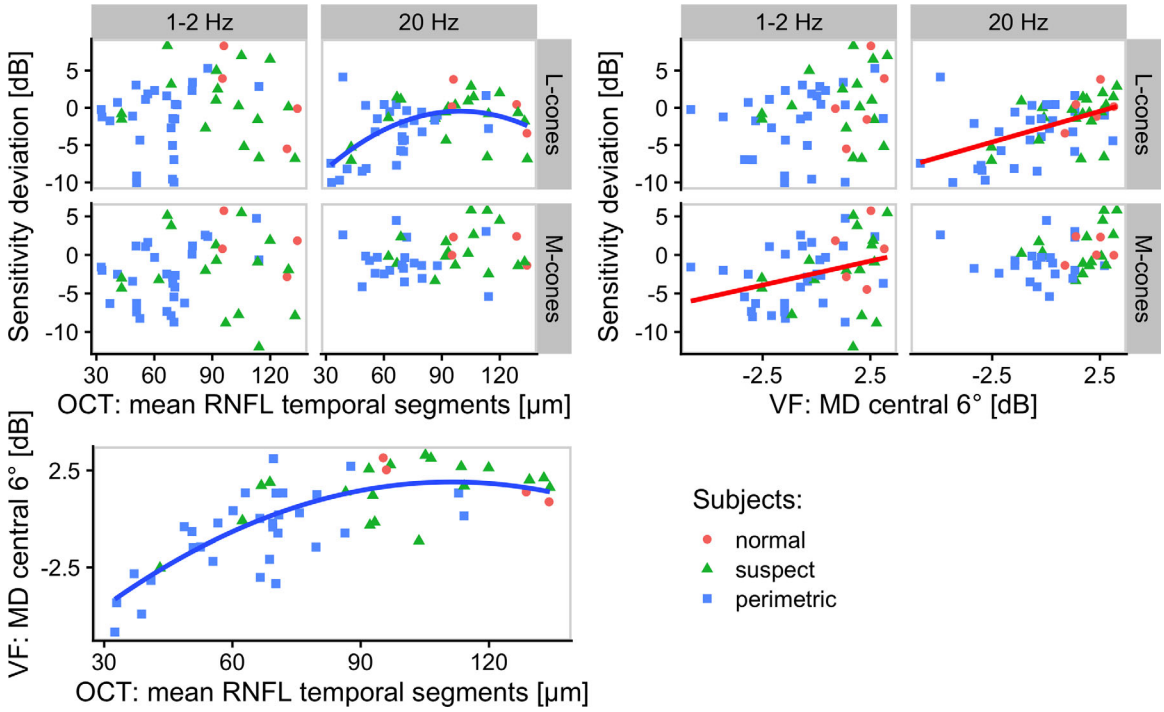

Figure 6. Relationship between photoreceptor-specific sensitivity deviation and the clinical parameters central visual field and temporal RNFL thickness (both cohorts). At 1 to 2 Hz, perception is mediated by the P-, at 20 Hz by the M-pathway. There was a clear relationship between magnocellular L-cone-driven sensitivity deviation at 20 Hz and corresponding visual field $MD_{6\ degrees}$/OCT $RNFL_{6\ degrees}$. Magnocellular M-cone-driven sensitivities had a limited dynamic range. Parvocellular-driven sensitivities had a much higher variability and some glaucoma suspects with good visual fields/RNFL thickness had reduced logCS. Linear (*red*) or quadratic (*blue*) regression models are shown in the plots, if model parameters were significant after correction for multiple testing. The relationship between RNFL thickness and $MD_{6\ degrees}$ as well as the relationship between $RNFL_{6\ degrees}$ thickness and magnocellularly driven sensitivity deviation was best described by a quadratic regression. Furthermore, there was a linear correlation between $MD_{6\ degrees}$ and sensitivity deviation.

parameters, temporal contrast sensitivity for L-cone isolating stimuli at 20 Hz (M-pathway) was significantly reduced in patients with advanced glaucoma. Furthermore, exclusively this sensitivity was significantly correlated with perimetric $MD_{6\ degrees}$ (linear relationship) and $RNFL_{6\ degrees}$ (quadratic relationship).

Vector Addition Model

The vector addition model that we used has been validated in normal trichromats and in dichromats.[13,27,28] To our knowledge, we are the first to use a vector addition model to describe threshold data from patients with glaucoma. Alvarez et al.[32] have used an ellipsoid fit for analyzing increment (and decrement) thresholds in patients with glaucoma for different color mixtures (red-green and blue-yellow), hypothesizing that mixtures with mostly chromatic contrast were detected by the parvocellular and those with dominating luminance contrast by the magnocellular pathway. However, the fact that a vector summation model could explain the thresholds to all combinations of L- and M-cone stimuli in our experiments implies that perception at the used stimulus frequencies was mediated by only one pathway[13] because threshold contours would substantially deviate from an ellipse otherwise.[26] Therefore, it cannot be excluded that stimulus detection in the experiments by Alvarez et al. were always dominated by the magnocellular pathway, because their stimuli have a sudden onset.[44]

Changes in Model Parameters in Glaucoma

Temporal properties of summation of photoreceptor inputs in the retinal ganglion cells may conceivably be altered in glaucoma, because remodeling of the dendritic tree has been demonstrated in morphologic structures.[10,45] This is of clinical interest, because it might allow identification of ganglion cell damage before cell death. Previously, we have found evidence of altered ERG response phases in patients with glaucoma.[46] However, in the present study, we have not found relevant differences in the phase angle parameter of the vector summation model between groups. As a consequence, we propose that pure L- and M-cone-specific temporal contrast sensitivities can be used to quantify functional loss of the different retino-geniculate systems in glaucoma and used these stimuli for further analysis.

Is There Preferential Damage?

Direct comparison between P- and M-pathway mediated contrast sensitivity deviations showed stronger losses in the P-pathway. However, M-pathway related losses were better correlated with other clinical findings. Thus, it is difficult to interpret the P-pathway-related losses. It is interesting that other studies that also have used red-green contrast for isolation of the P-pathway have often found larger functional loss in the P- compared with the M-pathway.[21–23] We are reluctant to attribute this to premorphological damage, because we do not have an objective correlate in the patients with

good RNFL thickness and poor temporal contrast sensitivities, and because criterion bias cannot be fully ruled out.[47]

Some authors have tried to identify functional changes that correspond to the morphological changes in synaptic density of the retinal ganglion cells before cell death.[10,45] Battista, Badcock, and McKendrick[25] have not found altered spatial summation in glaucoma using a paradigm by Pokorny and Smith,[48] whereas Sun et al. have found differences in the M-pathway contrast gain with a very similar approach.[24] Such questions might be addressed by measuring light adaptation and spatial summation with a more refined version of our technique in the future.

Correlation With Clinical Parameters

We have found that M-pathway-driven L-cone defects correlate with perimetric MD in a linear and with RNFL thickness in a quadratic fashion. At least for SAP, this is not surprising, because SAP is a luminance detection task dominated by L-cones.[44] Casson et al.[39] have also found higher temporal frequencies (8 Hz and 16 Hz) to be more useful in (achromatic) temporal modulation perimetry. In agreement with our data, Zhang et al.[49] have found a relationship between functional magnetic resonance imagery (fMRI) activation of the magnocellular layers of the LGN and structural parameters. The relatively poor correlation between functional loss of the P-pathway and RNFL thickness should be addressed in future studies, while considering possible criterion bias.[47]

Commercially available solutions for isolating retinogeniculate channels are short-wavelength-automated perimetry[50] for the koniocellular system, high pass resolution perimetry (HPRP)[9] for the parvocellular system, and frequency-doubling perimetry,[8] flicker perimetry,[51] flicker-defined form,[52] and motion perimetry for the magnocellular system. Rarebit perimetry was not designed to isolate a specific retinogeniculate pathway, but the parvocellular system might conceivably be the neural substrate, because stimuli are small and the P-pathway has the highest resolution.[53] In contrast to our test, the presumably parvocellular mediated HPRP and rarebit perimetry do not use red-green color discrimination but rather spatial discrimination for isolation. While these tests offer a detailed spatial characterization, retinal adaptation differs between tests and isolation of the targeted pathway is not always as expected.[44,53] This might explain why direct comparisons of commercially available tests are often inconclusive.[54,55] Our technique offers the possibility to validate the quality of isolation during the actual measurements by fitting ellipses.

Limitations

One limitation of our study is the age difference between the diagnostic groups, because temporal contrast sensitivity decreases with age. However, we think that the age correction, derived in another study, is most probably sufficient to account for this effect.[40] However, even when we assumed stronger age effects, it did not influence the conclusions. Nevertheless, studying age matched populations may give more conclusive results.

Our technique cannot be used in patients with anomalous trichromacy, because the cone fundamentals do not apply.[31] In dichromats, temporal contrast sensitivities of the remaining cone type can be obtained.[12,27,39] Furthermore, these observers have reduced sensitivities at low temporal frequencies, because the parvocellular system is not chromatically sensitive,[12] According to our calculations, our paradigm should be relatively robust to polymorphisms of the L- and M-cone-opsin genes.[35,36] We excluded X-linked color vision defects using dedicated tests, but we have found that such defects can also be identified from the temporal contrast sensitivity measurements themselves.[12,35,39]

Another limitation is that the low frequency range was represented by different temporal frequencies in the two cohorts (2015 = 1 Hz, and 2017 = 2 Hz). However, we found before that the sensitivities are very similar at these frequencies.[12] Rod intrusion in the M-cone-isolating stimuli cannot completely ruled out[12,35] but is expected to be small at the used retinal illuminance.

In its current form, the technique that we used can only provide global measures of retinal sensitivity. However, the results of the current study can be used to develop a photoreceptor-specific modulation perimetry (or campimetry). This is not possible with current screens or perimeters. However, novel monitors or projectors with four or more spectrally different light sources offer the possibility to present photoreceptor specific stimuli, with high temporal precision and with fixed states of retinal adaptation, at different locations in the visual field.

Conclusions

Photoreceptor-specific temporal contrast sensitivities may be a useful and versatile research tool for investigation functional consequences of glaucomatous damage, because the measurements can be performed at a fixed mean luminance and chromaticity. Therefore, the influence of retinal adaptation can be studied independently. Temporal and spatial structure can also be varied without sacrificing comparability between different retino-geniculate mechanisms. Although we cannot conclude whether parvo- or magnocellular-driven stimuli are better for early diagnosis of glaucoma, our data indicate that magnocellular-driven stimuli are more closely related to the widely accepted structural and functional parameters.

Acknowledgments

Supported by German Research Council (DFG) Grants HU2340/1-1 to CH and KR1317/16-1 to JK. Research Grants from the Friedrich-Alexander-University Erlangen-Nürnberg (ELAN 11.03.15.1, IZKF Rotationsstelle).

Disclosure: **C. Huchzermeyer**, None; **F. Horn**, None; **R. Lämmer**, None; **C. Mardin**, None; **J. Kremers**, None

References

1. Coleman AL. Glaucoma. *Lancet*. 1999;354(9192):1803–1810.
2. Quigley HA, Broman AT. The number of people with glaucoma worldwide in 2010 and 2020. *Br J Ophthalmol*. 2006;90(3):262–267.
3. Heijl A, Leske MC, Bengtsson B, Hyman L, Bengtsson B, Hussein M. Reduction of intraocular pressure and glaucoma progression: results from the Early Manifest Glaucoma Trial. *Arch Ophthalmol*. 2002;120(10):1268–1279.
4. The Advanced Glaucoma Intervention Study (AGIS): 7. The relationship between control of intraocular pressure and visual field deterioration. The AGIS Investigators. *Am J Ophthalmol*. 2000;130(4):429–440.
5. Baltmr A, Duggan J, Nizari S, Salt TE, Cordeiro MF. Neuroprotection in glaucoma - Is there a future role? *Exp Eye Res*. 2010;91(5):554–566.

6. Sena DF, Lindsley K. Neuroprotection for treatment of glaucoma in adults. *Cochrane Database Syst Rev*. 2017;1:CD006539.
7. Wu Z, Medeiros FA. Recent developments in visual field testing for glaucoma. *Curr Opin Ophthalmol*. 2018;29(2):141–146.
8. Anderson AJ, Johnson CA. Frequency-doubling technology perimetry. *Ophthalmol Clin North Am*. 2003;16(2):213–225.
9. Chauhan BC. The value of high-pass resolution perimetry in glaucoma. *Curr Opin Ophthalmol*. 2000;11(2):85–89.
10. Weber AJ, Kaufman PL, Hubbard WC. Morphology of single ganglion cells in the glaucomatous primate retina. *Invest Ophthalmol Vis Sci*. 1998;39(12):2304–2320.
11. Dacey DM. Parallel pathways for spectral coding in primate retina. *Annu Rev Neurosci*. 2000;23:743–775.
12. Huchzermeyer C, Kremers J. Perifoveal L- and M-cone-driven temporal contrast sensitivities at different retinal illuminances. *J Opt Soc Am A*. 2016;33(10):1989.
13. Lee BB, Martin PR, Valberg A. The physiological basis of heterochromatic flicker photometry demonstrated in the ganglion cells of the macaque retina. *J Physiol*. 1988;404:323–347.
14. Quigley HA, Dunkelberger GR, Green WR. Chronic human glaucoma causing selectively greater loss of large optic nerve fibers. *Ophthalmology*. 1988;95(3):357–363.
15. Anderson RS, O'brien C. Psychophysical Evidence for a Selective loss of M Ganglion Cells in Glaucoma. *Vision Res*. 1997;37(8):1079–1083.
16. Silverman SE, Trick GL, Hart WM. Motion perception is abnormal in primary open-angle glaucoma and ocular hypertension. *Invest Ophthalmol Vis Sci*. 1990;31(4):722–729.
17. Ansari EA, Morgan JE, Snowden RJ. Psychophysical characterisation of early functional loss in glaucoma and ocular hypertension. *Br J Ophthalmol*. 2002;86(10):1131–1135.
18. Swindale NV, Fendick MG, Drance SM, Graham SL, Hnik P. Contrast sensitivity for flickering and static letters and visual acuity at isoluminance in glaucoma. *J Glaucoma*. 1996;5(3):156–169.
19. McKendrick AM, Badcock DR, Morgan WH. Psychophysical measurement of neural adaptation abnormalities in magnocellular and parvocellular pathways in glaucoma. *Invest Ophthalmol Vis Sci*. 2004;45(6):1846–1853.
20. McKendrick AM, Sampson GP, Walland MJ, Badcock DR. Contrast sensitivity changes due to glaucoma and normal aging: Low-spatial-frequency losses in both magnocellular and parvocellular pathways. *Invest Ophthalmol Vis Sci*. 2007;48(5):2115–2122.
21. Pearson P, Swanson WH, Fellman RL. Chromatic and achromatic defects in patients with progressing glaucoma. *Vision Res*. 2001;41(9):1215–1227.
22. Rauscher FG, Chisholm CM, Edgar DF, Barbur JL. Assessment of novel binocular colour, motion and contrast tests in glaucoma. *Cell Tissue Res*. 2013;353(2):297–310.
23. Antón A, Capilla P, Morilla-Grasa A, Luque MJ, Artigas JM, Felipe A. Multichannel functional testing in normal subjects, glaucoma suspects, and glaucoma patients. *Invest Opthalmol Vis Sci*. 2012;53(13):8386.
24. Sun H, Swanson WH, Arvidson B, Dul MW. Assessment of contrast gain signature in inferred magnocellular and parvocellular pathways in patients with glaucoma. *Vision Res*. 2008;48(26):2633–2641.
25. Battista J, Badcock DR, McKendrick AM. Spatial summation properties for magnocellular and parvocellular pathways in glaucoma. *Invest Ophthalmol Vis Sci*. 2009;50(3):1221–1226.
26. Lee BB, Martin PR, Valberg A, Kremers J. Physiological mechanisms underlying psychophysical sensitivity to combined luminance and chromatic modulation. *J Opt Soc Am A*. 1993;10(6):1403–1412.
27. Kremers J, Usui T, Scholl HP, Sharpe LT. Cone signal contributions to electroretinograms [correction of electrograms] in dichromats and trichromats. *Invest Ophthalmol Vis Sci*. 1999;40(5):920–930.
28. Kremers J, Lee BB, Kaiser PK. Sensitivity of macaque retinal ganglion cells and human observers to combined luminance and chromatic temporal modulation. *J Opt Soc Am A*. 1992;9(9):1477–1485.
29. Donner KO, Rushton WAH. Retinal stimulation by light substitution. *J Physiol*. 1959;149(2):288–302.
30. Estevez O, Spekreijse H. The "silent substitution" method in visual research. *Vision Res*. 1982;22(6):681–691.
31. Shapiro AG, Pokorny J, Smith VC. Cone-rod receptor spaces with illustrations that use CRT phosphor and light-emitting-diode spectra. *J Opt Soc Am A Opt Image Sci Vis*. 1996;13(12):2319–2328.
32. Alvarez SL, Pierce GE, Vingrys AJ, Benes SC, Weber PA, King-Smith PE. Comparison of red-green, blue-yellow and achromatic losses in glaucoma. *Vision Res*. 1997;37(16):2295–2301.
33. Huchzermeyer CRH, Haubner S, Laemmer R, Mardin CY, Kremers JJ. Temporal contrast sensitivities are locally reduced around 4Hz for L-cone- and around 10Hz for M-cone isolating stimuli in glaucoma patients. *Invest Ophthalmol Vis Sci*. 2016;57(12):3941–3941.
34. Huchzermeyer CRH, Mardin CY, Lämmer R, Kremers JJ. Combining L- and M-cone-isolating stimuli to measure parvo- and magnocellular function in normal subjects and glaucoma patients. *Invest Ophthalmol Vis Sci*. 2019;60(9):2447–2447.
35. Huchzermeyer C, Kremers J. Perifoveal S-cone and rod-driven temporal contrast sensitivities at different retinal illuminances. *J Opt Soc Am A*. 2017;34(2):171.
36. Pokorny J, Smithson H, Quinlan J. Photostimulator allowing independent control of rods and the three cone types. *Vis Neurosci*. 2004;21(3):263–267.
37. Puts MJH, Pokorny J, Quinlan J, Glennie L. Audiophile hardware in vision science; the soundcard as a digital to analog converter. *J Neurosci Methods*. 2005;142(1):77–81.
38. Nygaard RW, Frumkes TE. Calibration of the retinal illuminance provided by Maxwellian views. *Vision Res*. 1982;22(4):433–434.
39. Huchzermeyer C, Martins CMG, Nagy B, et al. Photoreceptor-specific light adaptation of critical flicker frequency in trichromat and dichromat observers. *J Opt Soc Am A*. 2018;35(4):B106–B113.
40. Huchzermeyer C, Fars J, Kremers J. Photoreceptor-specific loss of perifoveal temporal contrast sensitivity in retinitis pigmentosa. *Transl Vis Sci Technol*. 2020;9(6):27.
41. Smith VC, Pokorny J, Davis M, Yeh T. Mechanisms subserving temporal modulation sensitivity in silent-cone substitution. *J Opt Soc Am A Opt Image Sci Vis*. 1995;12(2):241–249.
42. Marín-Franch I, Swanson WH. The visualFields package: a tool for analysis and visualization of visual fields. *J Vis*. 2013;13(4):10.
43. Garway-Heath DF, Holder GE, Fitzke FW, Hitchings RA. Relationship between electrophysiological, psychophysical, and anatomical measurements in glaucoma. *Invest Ophthalmol Vis Sci*. 2002;43(7):2213–2220.
44. Swanson WH, Sun H, Lee BB, Cao D. Responses of primate retinal ganglion cells to perimetric stimuli. *Invest Ophthalmol Vis Sci*. 2011;52(2):764–771.
45. Weber AJ, Harman CD. Structure–function relations of parasol cells in the normal and glaucomatous primate retina. *Invest Ophthalmol Vis Sci*. 2005;46(9):3197–3207.

Investigative Ophthalmology & Visual Science

46. Barboni MTS, Pangeni G, Ventura DF, Horn F, Kremers J. Heterochromatic flicker electroretinograms reflecting luminance and cone opponent activity in glaucoma patients. *Invest Ophthalmol Vis Sci*. 2011;52(9):6757–6765.
47. Rubinstein NJ, Turpin A, Denniss J, McKendrick AM. Effects of criterion bias on perimetric sensitivity and response variability in glaucoma. *Transl Vis Sci Technol*. 2021;10(1):18–18.
48. Pokorny J, Smith VC. Psychophysical signatures associated with magnocellular and parvocellular pathway contrast gain. *J Opt Soc Am A Opt Image Sci Vis*. 1997;14(9):2477–2486.
49. Zhang P, Wen W, Sun X, He S. Selective reduction of fMRI responses to transient achromatic stimuli in the magnocellular layers of the LGN and the superficial layer of the SC of early glaucoma patients. *Hum Brain Mapp*. 2016;37(2):558–569.
50. Sample PA, Johnson CA, Haegerstrom-Portnoy G, Adams AJ. Optimum parameters for short-wavelength automated perimetry. *J Glaucoma*. 1996;5(6):375–383.
51. Casson EJ, Johnson CA, Shapiro LR. Longitudinal comparison of temporal-modulation perimetry with white-on-white and blue-on-yellow perimetry in ocular hypertension and early glaucoma. *J Opt Soc Am A*. 1993;10(8):1792.
52. Quaid PT, Flanagan JG. Defining the limits of flicker defined form: effect of stimulus size, eccentricity and number of random dots. *Vision Res*. 2005;45(8):1075–1084.
53. Frisén L. New, sensitive window on abnormal spatial vision: rarebit probing. *Vision Res*. 2002;42(15):1931–1939.
54. Sample PA, Medeiros FA, Racette L, et al. Identifying glaucomatous vision loss with visual-function-specific perimetry in the diagnostic innovations in glaucoma study. *Invest Ophthalmol Vis Sci*. 2006;47(8):3381–3389.
55. Corallo G, Iester M, Scotto R, Calabria G, Traverso CE. Rarebit perimetry and frequency doubling technology in patients with ocular hypertension. *Eur J Ophthalmol*. 2008;18(2):205–211.

Investigative Ophthalmology & Visual Science